Open charm studies at Belle

Valentina Zhukova[1,*]

[1]P.N. Lebedev Physical Institute of the Russian Academy of Sciences, Moscow, Russia

Abstract. We present the new results of measurements of the exlusive cross sections of the e^+e^- annihilation to charmed meson pairs as a function of ceneter-of-mass energy from the open charm threashold up to $\sqrt{s}$ = 6 GeV using initial state radiation technique. The analysis is based on a data sample collected by the Belle detector with an integrated luminosity of 951 fb^{-1}. The accuracy of the cross section measurement is increased by a factor of 2 in comparison with the first Belle study. We have performed the first angular analysis of the $e^+e^- \to D^{*\pm}D^{*\mp}$ process and decomposed this exclusive cross section into three components corresponding to the different D^* helicities.

1 Introduction

Inspite the numerous efforts of experimentalists and theorists, the nature and properties of vector charmonia states lying above the open charm threshold are not fully undersood yet. For a long time, the mass and width of such resonances were determined by analyzing the inclusive hadronic e^+e^- cross section. However, the parameters determined in such a way are model-dependent and they suffer with large statistical uncertainties. On the contrary, measurements of exclusive cross sections allow us to determine the masses and widths of charmonia vector states by model-independent methods and to extract the constants relating them with elastic channels with open charm. This will provide a means to obtain the information on vector charmonium wave functions and to test the phenomenological models of charmonia.

The first measurements of the exclusive e^+e^- cross sections to different open-charm final states were presented by Belle [2–7] and BaBar [8–10] using the initial state radiation (ISR) technique. The ISR process, in which a hard photon with a significant part of initial energy is emitted before e^+e^- annihilation, allows one to get center-of-mass energies below the energy of B-factory. The continuous energy spectrum of such radiation allows to study cross sections in a large energy range.

Accurate measurements of two body open charm final states were presented by CLEO [11] using an energy scan in the narrow range of 3.97-4.26 GeV. Moreover Belle has demonstrated that in the studied energy region the sum of the measured two body ($D^{(*)}\bar{D}^{(*)}$, $D_s^{(*)+}D_s^{(*)-}$, $\Lambda_c^+\Lambda_c^-$) and three body $D\bar{D}^{(*)}\pi$ cross sections saturates within errors the total hadronic cross section (after subtraction of the u, d, and s continuum) [12]. The main contribution to the inclusive cross section comes from the $D\bar{D}$, $D\bar{D}^*$, and $D^*\bar{D}^*$ final states so that it is very important to measure these processes accurately.

*e-mail: zhukova.valentina07@gmail.com

Recently the first attempt to extract the parameters of ψ states (in particular, their couplings to the open-charm channels) was presented from a combined coupled-channel fit to all exclusive open charm cross sections measured by BelleRef. [13]. Although the suggested approach provides a good overall description of the line shapes, reliable conclusions have not be made because of the limited statistical accuracy of the data and because of the absence of the experimental information on the three helicity amplitudes of the $D^*\bar{D}^*$ system.

Here we report a new measurement of the exclusive cross sections $e^+e^- \to D^{(*)}D^*$ as function of the center-of-mass energy near the $D^{(*)}D^*$ threshold with initial state radiation (charge-conjugate modes are included throughout this paper). The increased data sample collected by Belle, the improved track reconstruction, few additional D and D^* decay modes used in event reconstruction provided more accurate cross sections results. We also perform the first angular analysis of the $e^+e^- \to D^{*\pm}D^{*\mp}$ processes which allows to decompose explicitly the studied cross section into three components corresponding to different D^*'s helicities.

2 Data sample and Belle detector

The reported analysis is based on the data sample with the integrated luminosity of 951 fb^{-1} collected by the Belle detector [14] at the KEKB asymmetric energy e^+e^- collider at the energies of the $\Upsilon(4S)$ and $\Upsilon(5S)$ resonances and the nearby continuum [15].

The Belle detector is a large-solid-angle magnetic spectrometer that consists of a silicon vertex detector (SVD), a 50-layer central drift chamber (CDC), an array of aerogel threshold Cherenkov counters (ACC), a barrel-like arrangement of time-of-flight scintillation counters (TOF), and an electromagnetic calorimeter (ECL) composed of CsI(Tl) crystals located inside a superconducting solenoid coil that provides a 1.5 T magnetic field. An iron flux-return located outside of the coil is instrumented to detect K_L^0 mesons and to identify muons (KLM). A detailed description of the detector can be found in [14].

3 Method

To select signal events we use the partial reconstruction method eleborated by Belle [3]. We fully reconstruct only one charmed meson (D^{*+} for $e^+e^- \to D^{*+}D^{*-}$ or D^+ for $e^+e^- \to D^+D^{*-}$), the $\gamma_{\rm ISR}$ photon, and the slow pion from the decay of other D^{*-} meson. Such partial D^{*-} reconstruction without reconstruction of the $\bar{D}^0$ from the D^{*-} decays allows to significantly increase the overall efficiency by a factor of ~ 20 for $e^+e^- \to D^{*+}D^{*-}$ and ~ 10 for $e^+e^- \to D^+D^{*-}$, while the method allows to suppress the backgrounds down to a low level and to subtract the residual backgrounds reliably using the data.

For the signal events the spectrum of masses recoiling against the $D^{(*)+}\gamma_{\rm ISR}$ system

$$M_{\rm rec}(D^{(*)+}\gamma_{\rm ISR}) = \sqrt{(E_{\rm c.m.} - E_{D^{(*)}\gamma_{\rm ISR}})^2 - p^2_{D^{(*)}\gamma_{\rm ISR}}}, \quad (1)$$

peaks at the D^{*-} mass. Here $E_{c.m.}$ is the e^+e^- center-of-mass energy, $E_{D^{(*)+}\gamma_{\rm ISR}}$ and $p_{D^{(*)+}\gamma_{\rm ISR}}$ are the center of mass energy, and momentum of the reconstructed $D^{(*)+}\gamma_{\rm ISR}$ system, respectively. According to Monte Carlo (MC) study, this peak is wide ($\sigma \sim 150$MeV/c^2) and asymmetric due to the asymmetric photon energy resolution function and higher order ISR corrections (*i.e.* more than one $\gamma_{\rm ISR}$ in the event). Because of poor $M_{\rm rec}(D^{(*)+}\gamma_{\rm ISR})$ resolution the signals from $D\bar{D}$, $D\bar{D}^*$, and $D^*\bar{D}^*$ strongly overlap, hence one cannot separate these processes using this selective variable only.

To resolve this problem we use the information provided by the slow pion from the unreconstructed D^{*-} meson. The distribution of the difference between the masses recoiling

against the $D^{(*)+}\gamma_{\rm ISR}$ and $D^{(*)+}\pi^-_{\rm slow}\gamma_{\rm ISR}$ (recoil mass difference),

$$\Delta M_{\rm rec} = M_{\rm rec}(D^{(*)+}\gamma_{\rm ISR}) - M_{\rm rec}(D^{(*)+}\pi^-_{\rm slow}\gamma_{\rm ISR}), \quad (2)$$

has a narrow peak for the signal process around the $m^{*+}_D - m_{D^0}$ mass difference. The resolution of this peak is better than 2 MeV/c^2 since the uncertainty of $\gamma_{\rm ISR}$ momentum is mostly canceled out for this variable. Thus the existence of a partially reconstructed D^{*-} in the event is identified by the presence of this peak. The method does not exclude contribution to the $\Delta M_{\rm rec}$ peak from processes with extra neutrals in the final state (*e.g.* $e^+e^- \to D^{(*)}D^*\pi^0$). However this background is suppressed and its residual contribution can be reliably determined using the data, as discussed below.

Usually for analising ISR procsses we required the fully reconstruction of the hadronic final state and $\gamma_{\rm ISR}$ is inferred from the spectrum of masses recoiling against the hadronic system. But here we require the reconstruction of the $\gamma_{\rm ISR}$. In spite of tendency to emit ISR photon outside the detector acceptance, the requirement to reconstruct $\gamma_{\rm ISR}$ does not significantly decrease the efficiency as slow pions from $D^{*\pm}$ decays have extremely low reconstruction efficiency when $\gamma_{\rm ISR}$ is outside the detector acceptance because of very low $p_\perp$ of $D^{(*)}D^*$ system in this case. Thus, if the ISR photon is emited along the beam pipe and undetected, the hadronic part of the ISR event can not be reconstructed as well.

To measure the exclusive cross sections as a function of $\sqrt{s}$ one needs to obtain the $D^{(*)}D^*$ mass spectrum. In the absence of higher-order QED processes, when one of D^* mesons remains unreconstructed the $D^{(*)}D^*$ mass corresponds to the mass recoiling against the single ISR photon: $M(D^{(*)}D^*) \equiv M_{\rm rec}(\gamma_{\rm ISR})$. However, the poor $M_{\rm rec}(\gamma_{\rm ISR})$ resolution ($\sigma \sim 120$MeV/c^2) does not allow the study of relatively narrow charmonium states in the $D^{(*)}D^*$ mass spectra. To improve the $M_{\rm rec}(\gamma_{\rm ISR})$ resolution we refit the recoil mass against the $D^{(*)+}\gamma_{\rm ISR}$ system, constrained to the D^* mass. This procedure utilizes the well-measured momentum of the reconstructed $D^{(*)+}$ meson to correct the momentum of the ISR photon. As a result, the $M_{\rm rec}(\gamma_{\rm ISR})$ resolution is drastically improved: near the threshold the resolution is better than 3 MeV/c^2, and smoothly increases up to 15 MeV/c^2 at $\sqrt{s} \sim 6$ GeV. The resolution of the recoil mass difference after refit, $\Delta M^{fit}_{\rm rec}$, improves also by a factor of ~ 2, which is exploited for more effective suppression of the combinatorial background.

In the previous Belle analysis, the strategy was to select a clean sample of the studied process with a minimal background contribution. The aim of the present analysis is to improve the accuracy of the cross section measurement. Here we use the advantages of technique elaborated in previous Belle analysis [3] and reoptimize the selection criteria and add more D decay modes to increase statistic.

4 Backgrounds

The following background sources were considered: (1) combinatorial $D^{(*)+}$ candidate combined with a true slow pion from D^{*-} decay; (2) real $D^{(*)+}$ mesons combined with a combinatorial slow pion; (3) both $D^{(*)+}$ and $\pi^-_{\rm slow}$ are combinatorial; (4a) reflection from the processes $e^+e^- \to D^{(*)+}D^{*-}\pi^0_{miss}\gamma_{\rm ISR}$ with a lost π^0 in the final state, including $e^+e^- \to D^{*+}D^{*-}\gamma_{\rm ISR}$ followed by $D^{*+} \to D^+\pi^0$; (4b) reflection from $e^+e^- \to D^{*+}D^{*-}\gamma_{\rm ISR}$ followed by $D^{*+} \to D^+\gamma$; (5)contribution from $e^+e^- \to D^{(*)+}D^{*-}\pi^0_{\rm fast}$, where the fast $\pi^0_{\rm fast}$ is misidentified as $\gamma_{\rm ISR}$.

The contribution from the combinatorial backgrounds (1)-(3) is extracted using two-dimensional sideband regions of the $D^{(*)+}$ candidate mass versus the recoil mass difference. The dominant part of the background (4) suppressed by tight requirement on $M_{\rm rec}(D^{(*)+})\gamma_{\rm ISR}$. The remaining part is estimated from the data measuring the isospic-conjugated process $e^+e^- \to D^{(*)0}D^{*-}\pi^+\gamma_{\rm ISR}$. We applied the similar partial reconstruction method by replacing

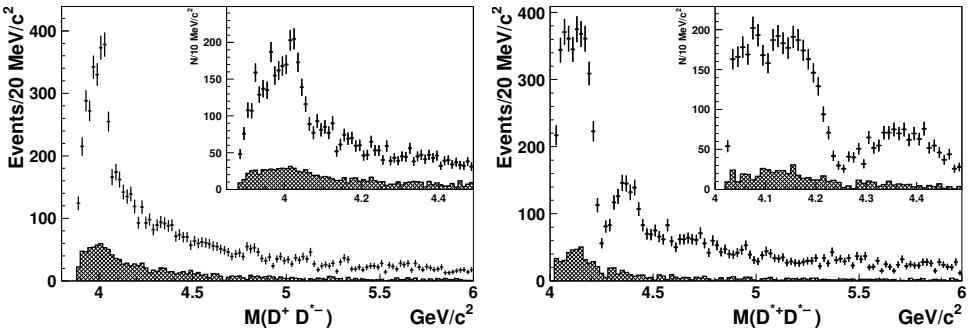

Figure 1. The a) D^+D^{*-} and b) $D^{*+}D^{*-}$ mass spectra in the data after applying all selection criteria (points with error bars). The sum of backgrounds (1)–(3) is shown as the hatched histogram. The inset shows the spectrum near the threshold with finer bins.

$D^{(*)+}$ with $D^{(*)0}$. Background (5) is estimated similarly to the study of $e^+e^- \to D^{(*)+}D^{*-}\gamma_{\rm ISR}$ (by replacing $\gamma_{\rm ISR}$ with $\pi^0_{\rm fast}$) and found to be negligibly small. Its possible contribution is included into the systematic uncertainty.

The obtained D^+D^{*-} and $D^{*+}D^{*-}$ mass spactra, after appling all requirements, are shown in Fig. 1.

5 Cross sections

We calculate the exclusive cross sections of the processes $e^+e^- \to DD^*$ and $e^+e^- \to D^*D^*$ as a function of $\sqrt{s}$ according to the formula:

$$\sigma_{e^+e^- \to D^{(*)}D^*} = \frac{dN/dM}{\eta_{\rm tot}(M) \cdot dL/dM} \tag{3}$$

where M is the $D^{(*)}D^*$ mass, equivalent to $\sqrt{s}$, dN/dM is the measured $M(D^{(*)}D^*)$ mass spectrum, $\eta_{\rm tot}$ is a M-dependent total efficiency, and dL/dM is the differential luminosity, caluclated theoretically up to the second order QED corrections [16].

Finally, the obtained exclusive $e^+e^- \to DD^*$ and $e^+e^- \to D^*D^*$ cross sections are shown in Fig. 2.

6 Angular analysis

We analyzed the $D^{*\pm}$ helicities for both $e^+e^- \to D^+D^{*-}\gamma_{\rm ISR}$ and $e^+e^- \to D^{*+}D^{*-}\gamma_{\rm ISR}$ processes. The $D^{*\pm}$ helicity angle, θ, is defined as the angle between the $\pi^\pm_{\rm slow}$ from $D^{*\pm}$ decay and the $D^{(*)+}D^{*-}$ system, seen from the $D^{*\pm}$ rest frame.

For the $e^+e^- \to DD^*$ process the helicity of the D^{*-} meson is uniquely defined by the angular momentum and parity conservation: the D^{*-} meson polarization should be transverse (T). Thus we perform the $D^{*\pm}$ angular analysis for this process to verify the method only. The longitudinal component (L) of the cross section is consistent with 0, as expected (Fig. 3).

The helicity composition of the D^*D^* final state is a mixture of TT, TL and LL components. We perform an analysis of the D^{*-} helicity angle in each bin of $M(D^*D^*)$.

The angular fit results are presented in Fig. 4. The cross sections corresponding to the different D^*D^* helicities have different $\sqrt{s}$-dependence. Near the threshold, the TT and TL

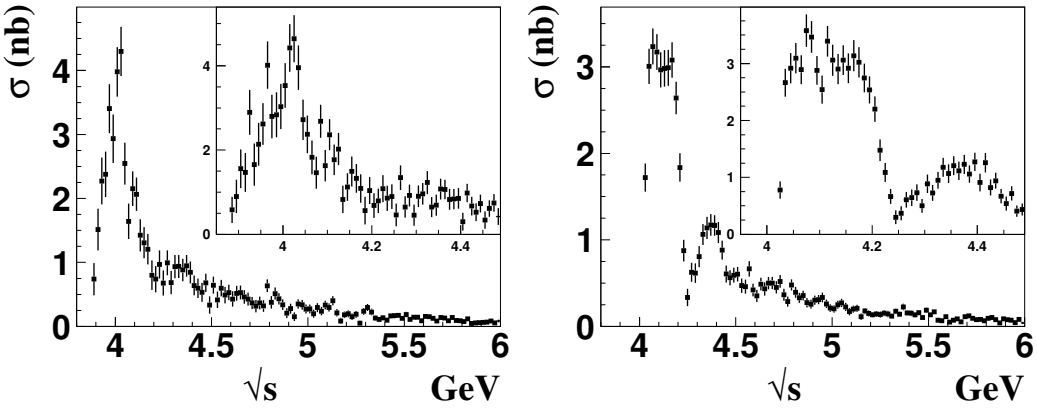

Figure 2. The exclusive cross sections as functions of $\sqrt{s}$ for $e^+e^- \to D^+D^{*-}$ (left) and $e^+e^- \to D^{*+}D^{*-}$ (right). The insets show the zoomed spectrum near the threshold with a half-size bin width.

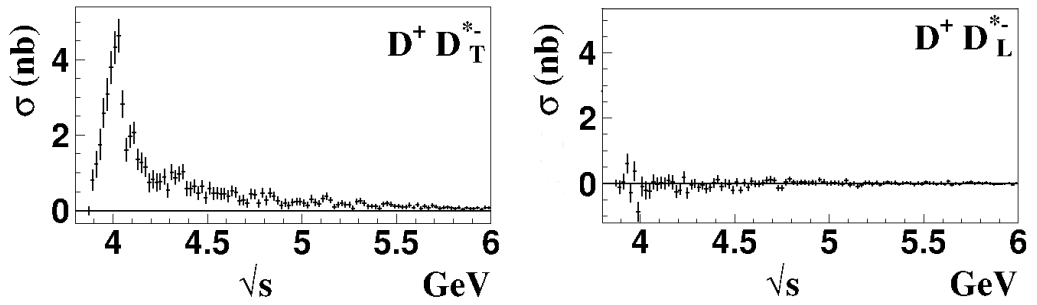

Figure 3. The components of the $e^+e^- \to D^+D^{*-}\gamma_{\rm ISR}$ cross section corresponding to the different D^{*-} helicity: left is transverse; right is longitudinal.

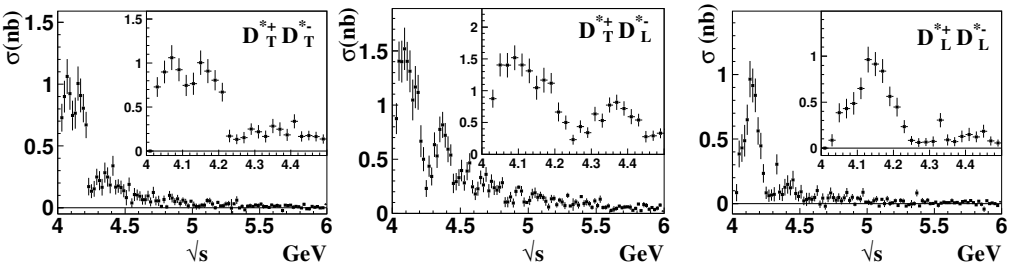

Figure 4. The components of the $e^+e^- \to D^*D^*\gamma_{\rm ISR}$ cross section corresponding to the different $D^{*\pm}$'s helicities. The insets show the zoomed spectrum near the threshold with a half-size bin width.

components have a similar sharp rise, while the LL component rises slowly. This can be explained by the higher centrifugal barrier for the LL component which originates from F wave [1] (chapter 48). Only the TL component survives in the region of high $\sqrt{s} > 4.5$ GeV, which is in good agreement with theoretical predictions [17].

7 Summary

In summary, we present a new measurements of the exclusive $e^+e^- \to D^+D^{*-}$ and $e^+e^- \to D^{*+}D^{*-}$ cross sections at $\sqrt{s}$ near D^+D^{*-} and $D^{*+}D^{*-}$ thresholds with initial state radiation. The accuracy of this cross section measurements is increased by a factor of 2 in comparison with the previous Belle results [3] due to increased data sample, improved track reconstruction efficiency and additional modes for the charmed meson reconstruction. The systematic uncertainties are significantly improved. We extend the energy region up to $\sqrt{s} = 6$ Gev, and taking advantage of the improved resolution and high statistics, decrease the size of the $\sqrt{s}$ steps close to threshold by a factor of two.

The complex shape of the $e^+e^- \to D^{*+}D^{*-}$ cross section can be explained by the fact that its components can reinforce or reduce each other. The fit of this cross section is not trivial, because it must take into account the threshold and coupled channels effects [13].

The first angular analysis of the $e^+e^- \to D^{*+}D^{*-}$ process allows to decompose the corresponding exclusive cross section into three components for the longitudinally and transversely polarized $D^{*\pm}$ mesons. The obtained components have different behavior near the $D^{*+}D^{*-}$ threshold. The only non-vanishing component at higher energy is the TL helicity of the $D^{*+}D^{*-}$ final state. The measured decomposition allows measurement of the couplings of vector charmonium states into different helicity components, useful to identify their nature and to test the heavy quark symmetry [18].

Acknowledgement We acknowledge support from the Russian Foundation for Basic Research No. 18-32-00091 and No. 17-02-00485.

References

[1] C. Patrignani *et al.* (Particle Data Group), Chin. Phys. C **40**, 100001 (2016).
[2] G. Pakhlova *et al.* (Belle Collaboration), Phys. Rev. D **77**, 011103 (2008).
[3] K. Abe *et al.* (Belle Collaboration), Phys. Rev. Lett. **98**, 092001 (2007).
[4] G. Pakhlova *et al.* (Belle Collaboration), Phys. Rev. Lett. **100**, 062001 (2008).
[5] G. Pakhlova *et al.* (Belle Collaboration), Phys. Rev. Lett. **101**, 172001 (2008).
[6] G. Pakhlova *et al.* (Belle Collaboration), Phys. Rev. D **80**, 091101 (2009).
[7] G. Pakhlova *et al.* (Belle Collaboration), Phys. Rev. D **83**, 011101 (2011).
[8] B. Aubert *et al.* (BaBar Collaboration), Phys. Rev. D **76**, 111105 (2007).
[9] B. Aubert *et al.* (BaBar Collaboration), Phys. Rev. D **79**, 092001 (2009).
[10] P.A. Sanchez *et al.* (BaBar Collaboration), Phys. Rev. D **82**, 052004 (2010).
[11] D. Cronin-Hennessy *et al.* (CLEO Collaboration), Phys. Rev. D **80**, 072001 (2009).
[12] A. J. Bevan *et al.* (BaBar and Belle Collaborations), Eur. Phys. J. C **74**, 3026 (2014).
[13] T. V. Uglov, Y. S. Kalashnikova, A. V. Nefediev, G. V. Pakhlova and P. N. Pakhlov, JETP Letters **105**, 1, 3 (2017)
[14] A. Abashian *et al.* (Belle Collaboration), Nucl. Instr. and Meth. A **479**, 117 (2002).
[15] S. Kurokawa, E. Kikutani, Nucl. Instr. and Meth. A **499**, 1 (2003); and other papers included in this volume.
[16] S. Actis *et al.* "Quest for precision in hadronic cross sections at low energy: Monte Carlo tools vs. experimental data", Eur. Phys. J. C **66**, 585-686 (2010)
[17] A.G. Grozin and M. Neubert, Phys. Rev. D **55**, 272 (1997).
[18] H. Georgi, "Heavy Quark Effective Field Theory", in: Proc. of the Theoretical Advanced Study Institute 1991, eds. R. K. Ellis, C.T. Hill, and J.D. Lykken (World Scientific, Singapore, 1992) p. 589